Vibration of a rectangular plate with a central power-law profiled groove by the Rayleigh-Ritz method

Vibration of a rectangular plate with a central power-law profiled groove by the Rayleigh–Ritz method

D.J. O'Boy *, V.V. Krylov

Department of Aeronautical and Automotive Engineering, Loughborough University, Leicestershire, UK

ABSTRACT

The prediction of natural frequencies of rectangular plates where a profiled indentation is present is made using a Rayleigh–Ritz variational energy method. Panels with holes are often found for access cables and access gaps, and it is shown that the application of damping to the profile leads to a more efficient method of reducing vibration than covering a whole rectangular plate, which is advantageous where weight saving is necessary.

© 2015 The Authors. Published by Elsevier Ltd. This is an open access article under the CC BY license (http://creativecommons.org/licenses/by/4.0/).

1. Introduction

A significant amount of research has been undertaken into the study of structural vibrations and methods to reduce the resonant amplitudes, including analyses which determine how to modify the structure to avoid coupling resonant frequencies with excitation sources, incorporating damping materials or the inclusion of special geometries to attenuate energy at specified frequencies [1]. More emphasis is also now placed on the optimisation of the design, in terms of the placement of the natural frequencies [2] and reducing the amount of damping material, in order to decrease the carbon footprint and installation time.

Many structural plate elements are formed from rectangular plates with various shapes machined into them, either for mass reduction or so that access holes are present for cables or control boxes. There is then the problem of determining the natural frequencies and minimising the coupling of different resonances. In order to reduce the vibration amplitude, damping material with a high stiffness and loss factor can be attached to the plate surface. A significant amount of the literature on thick and thin plates is available for regular shapes, see for example the work of Leissa [3,4] or Liew et al. [5].

When part of a structure containing flexural waves tapers to a sharp point, care must be taken in a finite element representation

[6] to avoid errors. For example, as the local flexural wavenumber at a position increases, the nodal density must also increase (this rapid increase in mesh density is computationally undesirable) and without the variation in mesh density, either the whole structure must be meshed to an extremely high fidelity (computationally significantly undesirable) or the finite element representation at the local position will be incorrect. In this paper, a relatively simple method is used to obtain the natural frequencies of a plate which has a section where the thickness varies with position using a continuous integration. While few papers consider the variation of thickness with position [7], even fewer consider the inclusion of variable thickness sections into constant thickness plates, see O'Boy et al. for examples [8,9], despite the interesting engineering applications for such plate structures. The aim of this paper is to illustrate how simple designs for plates with indentations may be tested rapidly with good accuracy using existing methods.

1.1. Vibration advantages for plates with profiled indentations.

It has previously been shown that a profiled indentation can be attached to a plate edge which can yield a greater loss factor for flexural vibrations, especially at higher mode numbers (a more efficient damping method) [8]. Although higher attenuation was obtained, the rectangular plate was left with a sharp edge which is relatively weak. By incorporating the tapering thickness into the centre of a structure, where access holes are required for cables/ conduits, this disadvantage can be overcome.

---

* Corresponding author.
   E-mail address: d.j.oboy@lboro.ac.uk (D.J. O'Boy).

When a flexural wave travels into a plate where the thickness is reduced, the amplitude of vibration increases and the phase speed of the wave decreases. There exist a limited number of mathematical profiles where analytical solutions to the simplified bending plate equation of motion can be found, one such group is a power-law profile, where the thickness varies according to $h(x) = \epsilon x^\gamma$, where γ and ϵ are positive constants. In beams for example, an analytical solution involving Bessel's functions is available for the case of a linear tapered profile [10] ($\gamma = 1$) but higher powers require a numerical approximation, while Mironov [11] has shown that the group velocity of a wave moving towards the end of the beam $x = 0$ asymptotically decreases to zero, when the power-law is $\gamma \geqslant 2$. It therefore never reaches the end and cannot reflect back from the free edge of the beam. When a truncation to the profile is included, the reflection coefficient again increases, but this can be negated through the application of polymeric damping layers [12,13]. As the incident flexural wave travels into the profile, the decreased thickness of material results in larger amplitude displacement away from the neutral layer and the damping material is extended and compressed at an amplified rate.

The application of thin damping layers to beam and plate structures is a well known damping method [14,15], however, the integration of a specified change in thickness as a means of reducing reflections from free edges is a novel concept. This tapering of the thickness has been reported as a viable means of reducing vibration, where the thickness of a section of a rectangular or cylindrical plate is reduced according to the power-law profile, where $\gamma \geqslant 2$. Experimental measurements and numerical predictions were carried out on a rectangular plate with and without a wedge of quadratic power-law profile added to one side, as shown in Fig. 1. It was shown that when a layer of damping tape was applied to the plain plate, only a reduction of 1–5 dB of cross-point mobility amplitude was found. When the damping tape was applied to the wedge profile, a reduction of 10–15 dB was found [8].

In this paper, a simple Rayleigh–Ritz variational model is documented which determines the vibration characteristics of an asymmetric or symmetric profile into a rectangular plate in any arbitrary position, such as Fig. 2. The first natural frequency is predicted for the case of a double groove machined into the centre of the plate, utilising both linear and quadratic power-laws, of varying sizes, to an accuracy which would be acceptable for use by most design requirements.

The numerical Rayleigh–Ritz variational model is detailed in Section 2, both for a constant thickness plate and the modifications required for the addition of a profiled section. Then, numerical results are shown in Section 2.3 with comparisons to the other results in the literature, as a means of validation of the methods used.

In Section 3, the numerical method is then used to predict the first natural frequency for a range of plate dimensions, where the length of the tapering profiles are varied. An example of the industrial use of such plates with access holes, in terms of the damping of vibration, is provided in Section 4.
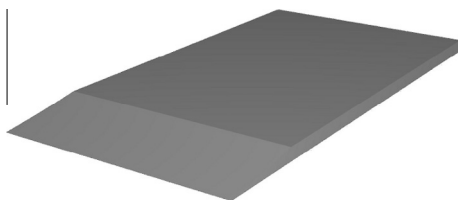
Fig. 1. Rectangular plate incorporating a quadratic wedge of power-law profile machined onto the end. Damping tape is applied to the very tip of the wedge.
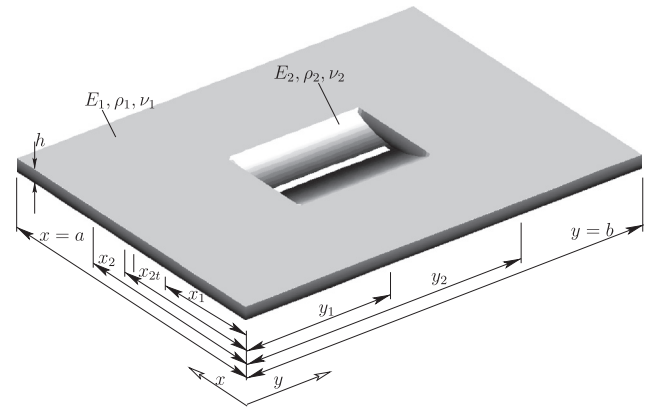
Fig. 2. Dimensions of the structural plate idealised in the numerical model, with a central quadratic power-law profile with truncation position leaving a gap in the centre of the plate.

1.2. Numerical solutions to plate vibration involving a change in thickness

The use of rectangular plates is widespread, many of which suffer from excessive vibration causing joint fatigue, tactile discomfort and acoustic problems [16] [17, pp. 2-42]. The behaviour of flexural and extensional plate vibrations has been explored by Mansfield [18] using infinite series solutions to determine the natural frequencies where the thickness varies exponentially and an annular plate where the thickness varies as a power of the radius, including a variation in temperature. Additional numerical solutions to variable thickness plates can also be found in Trapezon [19], Lardner [20] or Wang [21].

The most common numerical solutions to the vibration of tapered plates use this method of an infinite power series in the displacement function. Jain and Soni [22] have a thorough analysis of the free vibrations of rectangular plates where the thickness varies according to a parabolic curve. Tomar et al. [23] have also used a similar method to analyse the vibrations of an infinite plate with a linear variation in thickness, with results for the first two modes of vibration determined.

The Rayleigh–Ritz variational method has been applied to rectangular plates by a range of authors and the methods used in this paper build upon this work, adding to the literature, see for example Young [24] and Warburton [25] for rectangular plates or Gupta and Bhardwaj [26] for orthotropic elliptical plates (see also Chakraverty et al. [7] for a generalised method for inhomogeneous orthotropic circular plates). In order to remove a rectangular section of plate, the Ritz method by Laura et al. [27,28] will be employed and is applicable with the simple shape function used in this paper for a variety of rectangular aspect ratios, in different positions on the plate [29]. As the method is based on energy distribution in the plate, it readily lends itself to the analysis of complex plate shapes. It is not the intention to demonstrate the most efficient convergence, rather that complicated shapes can be obtained without recourse to more complicated techniques such as finite element.

2. Numerical model of a plate with a profiled section in the centre

A numerical model is required to determine the natural frequencies of three distinct plates; a plain rectangular plate, a plate with a square shouldered hole and a plate with a double quadratic power-law profile across the width of the plate, the subject of this paper illustrated in Fig. 2.

The overall plate has material properties of Young's modulus E_1 Pa, density ρ_1 kg/m³, Poisson's ratio v_1 and dimensions in (x, y) of (a, b) m respectively. The flexural displacement from the neutral layer is denoted by $w(x, y)$ m assuming harmonic vibration of frequency ω rad/s. The bending stiffness of the plate is $D_1 = E_1 h_1^3 / 12(1 - v_1^2)$ Nm where h_1 m is the constant thickness.

The Rayleigh–Ritz variational method is an energy method, so that a central rectangular section can be removed from this plate, to be replaced with another plate with properties denoted E_2, ρ_2, v_2 and thickness which varies with position $h_2(x, y)$. The properties of plate 1 will always be the same as plate 2 and the solutions gathered are the undamped natural frequencies.

2.1. Rayleigh–Ritz variational method for uniform plate vibration

The Rayleigh–Ritz variational method is documented by Young [24], although a simpler set of admissible functions are utilised, as also discussed by Warburton [30], which provides an

$$C_{mn}^{(ij)} = \begin{cases} D_1 \left\{ \int_0^a \int_0^b \left(\frac{\partial^2 X_m}{\partial x^2} \right)^2 Y_n^2 + X_m^2 \left(\frac{\partial^2 Y_n}{\partial y^2} \right)^2 \mathrm{d}x\,\mathrm{d}y + 2v_1[E_{mm}F_{nn}] + 2(1 - v_1)H_{mm}K_{nn} \right\} & \text{for} \quad mn = ij, \\ D_1 \{ v_1[E_{mi}F_{jn} + E_{im}F_{nj}] + 2(1 - v_1)H_{im}K_{jn} \} & \text{for} \quad mn \neq ij, \end{cases} \tag{7}$$

approximation of the natural frequencies and locations of nodal points for a given geometry by equating the maximum potential energy with the maximum kinetic energy at resonant frequencies. The maximum potential energy of the (constant thickness) plate flexural vibration is given by,

$$U_{\mathrm{Max}} = \frac{D_1}{2} \iint \left\{ \left(\frac{\partial^2 w}{\partial x^2} \right)^2 + \left(\frac{\partial^2 w}{\partial y^2} \right)^2 + 2v_1 \frac{\partial^2 w}{\partial x^2} \frac{\partial^2 w}{\partial y^2} \right.$$
$$\left. + 2(1 - v_1) \left(\frac{\partial^2 w}{\partial x \partial y} \right)^2 \right\} \mathrm{d}x\,\mathrm{d}y \tag{1}$$

and the maximum kinetic by,

$$T_{\mathrm{Max}} = \frac{1}{2} \rho_1 h_1 \omega^2 \iint w^2 \, \mathrm{d}x\,\mathrm{d}y. \tag{2}$$

The displacement is assumed to be an infinite series of admissible shape functions in the x and y directions. This numerical method constrains the total number of shape functions in the two directions to a maximum of M, N terms respectively, with amplitudes b_{mn}.

$$w(x, y, t) = \sum_{m=1}^{M} \sum_{n=1}^{N} X_m(x) Y_n(y) b_{mn} e^{i\omega t}. \tag{3}$$

When the series solution is substituted into Eqs. (1) and (2), an expression is obtained which is a function of the amplitudes b_{mn}. If the difference in the potential and kinetic energy is denoted J, then the Rayleigh–Ritz method requires the minimisation of J with respect to these amplitudes, obtained by taking the partial derivatives of J with respect to b_{mn} and setting equal to zero.

$$\frac{\partial J}{\partial b_{ij}} = 0 = \frac{\partial U_{\mathrm{Max}}}{\partial b_{ij}} - \frac{\partial T_{\mathrm{Max}}}{\partial b_{ij}}, \tag{4}$$

where the indices i, j represent any of m, n. This latter equation produces an $M \times N$ system of linear homogeneous equations in the unknown amplitudes b_{mn}. For a suitable set of orthogonal shape

functions, the matrices determining the natural frequencies of vibration may be written as,

$$\sum_{m=1}^{M} \sum_{n=1}^{N} [C_{mn}^{(ij)} - \lambda \delta_{mn}] b_{mn} = 0, \tag{5}$$

where $\lambda = \omega^2$ and for the case of a solid rectangular plate,

$$\delta_{mn} = \{ \rho_1 h_1 ab/4 \text{ for } mn = ij, \quad 0 \text{ for } mn \neq ij. \tag{6}$$

Two simple shape functions are implemented in this paper, $X(x) = \sin(m\pi x/a)$, $Y(y) = \sin(n\pi y/b)$, which completely satisfy the simply supported boundary conditions on the outer edges of the plates, but only approximate the edges on the inside of the plate. This is admissible when using the Rayleigh–Ritz method as the approximate boundary condition becomes more accurate as the number of terms in the series increases to infinity (subject to numerical considerations), see Larrondo et al. [31] who also employs a double Fourier series of shape functions to investigate a rectangular plate with a linear variation in thickness. The individual terms in the matrix are given by,

where

$$E_{im} = \int_0^a X_i \frac{\partial^2 X_m}{\partial x^2} \mathrm{d}x, \quad E_{mi} = \int_0^a X_m \frac{\partial^2 X_i}{\partial x^2} \mathrm{d}x, \quad F_{jn} = \int_0^b Y_j \frac{\partial^2 Y_n}{\partial y^2} \mathrm{d}y,$$
$$F_{nj} = \int_0^b Y_n \frac{\partial^2 Y_j}{\partial y^2} \mathrm{d}y, \quad H_{im} = \int_0^a \frac{\partial X_i}{\partial x} \frac{\partial X_m}{\partial x} \mathrm{d}x, \quad K_{jn} = \int_0^b \frac{\partial Y_j}{\partial y} \frac{\partial Y_n}{\partial y} \mathrm{d}y. \tag{8}$$

Eq. (5) takes the form of a secular determinant [24], with a separation of odd and even modes of vibration where these decouple [27,30] due to lines of symmetry. The numerical solution utilised a size for M and N of 30 terms to obtain both the resonant frequency for each mode number and also the mode shapes. The natural frequency for the plate is non-dimensionalised and represented by $\Omega = a^2 \omega \sqrt{\rho_1 h_1 / D_1}$.

2.2. Inclusion of a power-law profiled section in the plate

The numerical model must be able to calculate not just the natural frequencies of a rectangular plate, but the modifications which arise when a linear or quadratic power-law profile is machined in the plate centre, see Fig. 2. For the double profile along the coordinate x, it is assumed that it extends from x_1 to x_2, so that the thickness is given by $h(x) = \epsilon |(x - \alpha)|^\gamma$ m where the constant $\alpha = (x_1 + x_2)/2$ m locates the profile in the centre of the plate, $\gamma = 1$ for a linear wedge and $\gamma = 2$ for a quadratic profile.

The expressions for the maximum potential and kinetic energy are also valid where the plate thickness varies with the position, provided the varying bending stiffness in Eq. (1) is taken inside the integral and the integration is carried out over the whole plate area. Similarly, the change in thickness in the kinetic energy, Eq. (2) is also required to be calculated over the whole region of the integral, as detailed by Nallim et al. [32] through the application of the Rayleigh–Ritz method in polygonal plates with a linear variation in thickness.

The inclusion of a profiled section in the centre of the plate as shown in Fig. 2 requires the energy terms associated with a hole of dimensions ($x = x_1$ to x_2, $y = y_1$ to y_2) to be removed from

Eq. (5), and the energy terms associated with the profiled plate substituted in, these having bending stiffness D_2. The modified integrals E'_{im}, E'_{mi} are introduced and H'_{im} where the limits now exist between x_1 and x_2. Similarly in the y axis, the modified integrals are now F'_{jn}, F'_{nj} and K'_{jn} with limits from y_1 to y_2. Then following the procedure by Laura [33], the method to remove a central hole of the plate and replace it with a different constant thickness plate modifies the matrix element, Eq. (7) as follows,

$$
C_{mn}^{(mn)} = D_1 \left\{ \int_0^a \int_0^b \left(\frac{\partial^2 X_m}{\partial x^2} \right)^2 Y_n^2 + X_m^2 \left(\frac{\partial^2 Y_n}{\partial y^2} \right)^2 \mathrm{d}x\,\mathrm{d}y \right\}
$$
$$
- (D_1 - D_2) \left\{ \int_{x_1}^{x_2} \int_{y_1}^{y_2} \left(\frac{\partial^2 X_m}{\partial x^2} \right)^2 Y_n^2 + X_m^2 \left(\frac{\partial^2 Y_n}{\partial y^2} \right)^2 \mathrm{d}x\,\mathrm{d}y \right\}
$$
$$
+ 2 v_1 D_1 [E_{mm} F_{nn}] - 2[D_1 v_1 - D_2 v_2] [E'_{mm} F'_{nn}]
$$
$$
- 2[D_1(1 - v_1) - D_2(1 - v_2)] H'_{mm} K'_{nn}
$$
$$
+ 2D_1(1 - v_1) H_{mm} K_{nn} \quad \text{for} \quad mn = ij, \tag{9}
$$

$$
C_{mn}^{(ij)} = (D_2 - D_1) \left\{ \int_{x_1}^{x_2} \int_{y_1}^{y_2} \left(\frac{\partial^2 X_m}{\partial x^2} \right)^2 Y_n^2 + X_m^2 \left(\frac{\partial^2 Y_n}{\partial y^2} \right)^2 \mathrm{d}x\,\mathrm{d}y \right\}
$$
$$
+ D_1 v_1 [E_{mi} F_{jn} + E_{im} F_{nj}] - [D_1 v_1 - D_2 v_2] [E'_{mi} F'_{jn} + E'_{im} F'_{nj}]
$$
$$
- [2(1 - v_1)D_1 - 2(1 - v_2)D_2] H'_{im} K'_{jn} + 2(1 - v_1)D_1 H_{im} K_{jn}, \tag{10}
$$

$$
\delta_{mn} = \begin{cases} \rho_1 h_1 ab/4 - (\rho_1 h_1 - \rho_2 h_2) \int_{x_1}^{x_2} \int_{y_1}^{y_2} X_m^2 Y_n^2 \mathrm{d}x\,\mathrm{d}y & \text{for} \quad mn = ij, \\ -(\rho_1 h_1 - \rho_2 h_2) \int_{x_1}^{x_2} \int_{y_1}^{y_2} X_m^2 Y_n^2 \mathrm{d}x\,\mathrm{d}y & \text{for} \quad mn \neq ij. \end{cases} \tag{11}
$$

An analytical form of this integration (with the bending stiffness term inside the integral) is used at all times for this inner section based on the summation of each individual power of x with the shape function.

Finally, it is impossible to machine a power-law profile with such precision that it can extend to zero thickness, rather, in the manufacturing process, the profile is truncated at a position $x = x_{1t}$ on one side and at a position $x = x_{2t}$ on the other, where the length of the power-law profile can be manipulated by varying this truncation position in terms of the limits of the integration in Eqs. (10) and (11). The truncation is necessary for convergence, as discussed in Krylov [12], while Zhou describes the application of a boundary condition to a beam with a sharp point. It is pointed out that any solution found in this case would be inconsistent as the beam with a sharp point cannot sustain a bending moment or shear force and that the deflection is required to be finite at the end of the beam [34]. In the case of finite elements, the mesh density would still have to be increased significantly closer to the truncation point, even with the truncation. The analytical integration is efficient in this case.

2.3. Series convergence

Results are shown for a steel material, a Poisson's ratio of $v = 0.3$, with the convergence of natural frequency for a square plate ($a = b$) and central hole incorporating a linear and quadratic power-law profile in Fig. 3. The size of the central hole is given as a ratio a_1/a, b_1/b where $a_1 = x_2 - x_1$, $b_1 = y_2 - y_1$. The truncation position of the power-law profile is set at $(x_{2t} - x_{1t})/a = 0.1 a_1/a$.

The first mode is obtained with sufficient accuracy after approximately $M = N = 21$ terms. The following results in this paper are obtained with 30 terms, sufficient to resolve the change in resonant frequency to within one percent. As an example, a
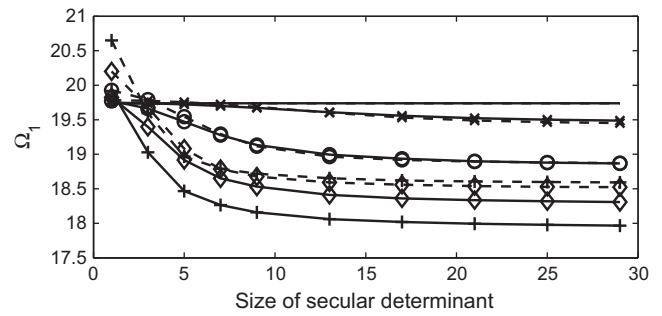
Fig. 3. Convergence of Ω_1 with increasing size of the secular determinant M, for the case of (solid line) a linear wedge and (dashed line) a quadratic wedge in a square plate with variously sized inner profile, $-$ $a_1/a = 0.0$, $-\times$ $a_1/a = 0.1$, $-o$ $a_1/a = 0.2$, $-\diamond$ $a_1/a = 0.3$, $-+$ $a_1/a = 0.4$. Truncation position at $(x_{2t} - x_{1t})/a = 0.1 a_1/a$.

square plate with a central hole $a_1/a = 0.2$ and truncation point $(x_{2t} - x_{1t})/a = 0.1 a_1/a$ with a linear wedge has first natural frequency $\Omega_1(M = N = 28) = 19.013$ and $\Omega_1(M = N = 30) = 19.008$, a reduction of 0.03 percent. For the case of a quadratic power-law, the convergence is $\Omega_1(M = N = 28) = 18.954$ and $\Omega_1(M = N = 30) = 18.949$, a reduction of 0.02 percent. Although this simple method always overestimates the resonant frequency through an upper bound, it still can provide an estimate to within acceptable accuracies for most engineering applications. For the ninth frequency, the reduction between 28 and 30 terms is 0.32 percent.

2.4. Validation

The variational method has been successfully used to predict the natural frequencies of a plate with a central square or rectangular hole, see for example the work of Laura et al. [27,28]. The method used in this paper does not differ in the mathematical approach, only the likely numerical implementation. The natural frequencies of a rectangular plate with rectangular central hole are provided in Table 1, where it may be seen that using $N = 30$ terms, the natural frequencies in [28] can be obtained (the variation is due to a different number of terms in the variational method).

It remains to provide a validation for the use of the variational Rayleigh–Ritz method for a thickness varying profile. The comparison is made with the finite element results published by Larrondo et al. [31] for a single linear rectangular wedge. In this case, the linear profile extends from $x = x_1 = 0$ to $x = x_{1t} = a$ (the second profile using dimensions x_2 and x_{2t} are not utilised), where the thickness variation $h(x) = \epsilon(\alpha - x)$ is dictated by the constant ζ, the taper constant $\epsilon = \zeta h_1/a$ and $\alpha = (1 + \zeta)a/\zeta$. The natural frequencies predicted by this paper for the range of taper geometries

Table 1
First non-dimensionalised natural frequency Ω_1 for a rectangular plate with rectangular hole. Values in brackets are given by Laura [28].

a_1/a	b/a				
	1.0	0.9	0.8	0.7	0.6
0.10	19.486	21.766	24.935	29.533	36.576
	(19.800)	(22.120)	(25.360)	(30.070)	(37.320)
0.20	19.169	21.396	24.456	28.837	35.459
	(19.630)	(21.920)	(25.070)	(29.610)	(36.500)
0.30	19.481	21.728	24.768	29.056	35.438
	(19.850)	(22.140)	(25.250)	(29.650)	(36.220)
0.40	20.788	23.166	26.334	30.727	37.155
	(21.150)	(23.570)	(26.810)	(31.310)	(37.930)
0.50	23.491	26.158	29.652	34.414	41.251
	(23.840)	(26.550)	(30.110)	(34.970)	(41.980)

Table 2

First natural frequency Ω_1 for a rectangular plate with a single linear taper in one direction only, simply supported on all edges. Validated results in brackets are finite element calculations given by Larrondo et al. [31].

b/a	ζ		
	0.2	0.5	0.8
4.00	11.508 (11.508)	12.958 (12.956)	14.335 (14.329)
2.00	13.549 (13.549)	15.302 (15.301)	16.995 (16.993)
1.00	21.692 (21.692)	24.557 (24.556)	27.363 (27.362)
0.50	54.161 (54.161)	61.010 (61.011)	67.537 (67.539)

and rectangular plate sizes are compared to the finite element calculations in Table 2 with excellent accuracy and agreement.

The energy method has been validated in stages against published results from the literature, showing that the method can be used to determine the plate shape for variable thickness sections, providing that the integrals in Eq. (10) can be completed successfully. In order to improve accuracy for the natural frequencies of the higher order modes, alternative shape functions in Eq. (3) and non-dimensionalised coordinates could be incorporated. For example, polynomial co-ordinate functions can yield excellent accuracy for the fundamental frequency in addition to allowing a simple integration method for the case of a non-linear thickness or inhomogeneous medium (note that in this paper, the shape function also allows a highly computationally efficient analytical integration method to be employed). Often the specific choice of shape functions is determined by the boundary conditions or numerical implementation [34].

3. Results

The natural frequencies are presented for various configurations of the plate with a profiled inclusion, including both square and rectangular plate sizes and various ratios a_1/a to vary the outer size of the profile. The truncation positions are also varied which has the effect of increasing or decreasing the overall size of the inner hole.

A table of results showing the variation of non-dimensionalised natural frequency for a square plate with a variable size inner hole containing a linear profile section is shown in Table 3 where the truncation position of the linear wedge is also altered. Varying the truncation position also varies the size of the inner aperture. The same comparison is produced for a quadratic power-law profile in Table 4.

It can be seen that the natural frequency of the plate with a linear wedge is generally higher than with a quadratic power-law profile for small inner profile sizes, as with the quadratic profile the material becomes thinner approximately half way down the wedge length, with the associated reduction in flexural stiffness. As the size of the inner profile is increased, the natural frequency varies, initially decreasing and then increasing. As the truncation

Table 3

First natural frequency Ω_1 for a square plate with profiled inner double linear profile. Variation of the size of the outer profile and truncation length.

a_1/a	$(x_{2t} - x_{1t})/a_1$					
	0.00	0.05	0.10	0.15	0.20	0.25
0.10	19.486	19.487	19.488	19.491	19.494	19.497
0.17	19.076	19.078	19.082	19.090	19.099	19.109
0.20	18.858	18.860	18.867	18.878	18.892	18.907
0.30	18.282	18.289	18.307	18.335	18.370	18.415
0.33	18.135	18.144	18.167	18.203	18.250	18.309
0.40	17.916	17.929	17.966	18.022	18.099	18.197
0.50	17.738	17.761	17.827	17.931	18.075	18.252

Table 4

First natural frequency Ω_1 for a square plate with profiled inner double quadratic power-law profile. Variation of the size of the outer profile and truncation length.

a_1/a	$(x_{2t} - x_{1t})/a_1$					
	0.00	0.05	0.10	0.15	0.20	0.25
0.10	19.453	19.453	19.453	19.453	19.454	19.455
0.17	19.057	19.057	19.058	19.059	19.061	19.064
0.20	18.871	18.871	18.872	18.873	18.877	18.882
0.30	18.521	18.521	18.523	18.528	18.537	18.551
0.33	18.495	18.496	18.498	18.504	18.516	18.535
0.40	18.588	18.589	18.593	18.604	18.623	18.654
0.50	19.048	19.050	19.059	19.081	19.122	19.185

positions are increased (increasing the aperture hole in the centre of the plate) the natural frequency decreases as the overall stiffness is decreased.

The vibration modes of the plate for higher natural frequencies are shown in Fig. 4 for a square plate with a double quadratic power-law profile, where the outer size of the power-law profile is $a_1/a = 0.2$ and the truncation position is $(x_{2t} - x_{1t})/a = 0.1 a_1/a$. It can be seen that the addition of a damped profile will especially influence the forced vibration amplitude of the second, sixth, seventh and ninth natural frequency, as the anti-nodal locations are located close to the profile, parallel to the axis of displacement where any amplified motion will cause compression and extension of any damping layer attached to the profile.

If the outer dimension of the power-law profile, $a_1/a = 0.2$ is maintained and the truncation position of the profiles are altered, the impact on the first natural frequencies can be seen in Fig. 5(a)–(c) for the case of a linear and quadratic power-law variation. The variation in frequency is much larger with the linear case than the quadratic, indicating that the trade-off between mass and flexural stiffness reduction is more sensitive in the former case. Interestingly the first natural frequency can be designed to be the same with either profile, although this possibility does not exist with the higher modes, as the truncated profile is not near any anti-nodes at these frequencies.

The variation in the natural frequency for the case where the outer and inner rectangular plates are rectangular rather than square are now presented. The case of a linear profile where $b/a < 1$ are shown in Table 5, whereas the case where the profile is larger, $b/a > 1$ is shown in Table 6.

The identical cases for a profile with a quadratic power-law variation is shown in Tables 7 and 8 for the case of $b/a < 1$ and $b/a > 1$ respectively. The trend of variation in frequency parameter where the ratio of the plate dimensions are altered agrees with the study by Jain and Soni, who also found that Ω increases with an increase in the a/b ratio [22].

4. Impact of a profiled inclusion on the damped natural frequencies

Damping added to the plate, which is consistent with typical industrial solutions to noise and vibration issues is now shown. It is assumed that the structure represents a panel with access holes for cables or conduits, see Fig. 6 for an example of an automotive panel with holes for weight saving.

The cases will be compared for a plate of dimension $(a, b) = (1.0, 0.5)$ m, with central inner profile size $(a_1, b_1) = (0.3, 0.3)$ m with reference to Fig. 2. The double profile is quadratic in the x direction with truncation points $(x_{t1}, x_{t2}) = (0.485, 0.515)$ m. The plate materials are considered to be rolled mild steel with Young's modulus, density and Poisson's ratio given by $E_1 = 190$ GPa, $\rho_1 = 7850$ kg/m^3 and $v = 0.3$ respectively. The inherent damping in the metal is approximated as $\eta = 0.01$.
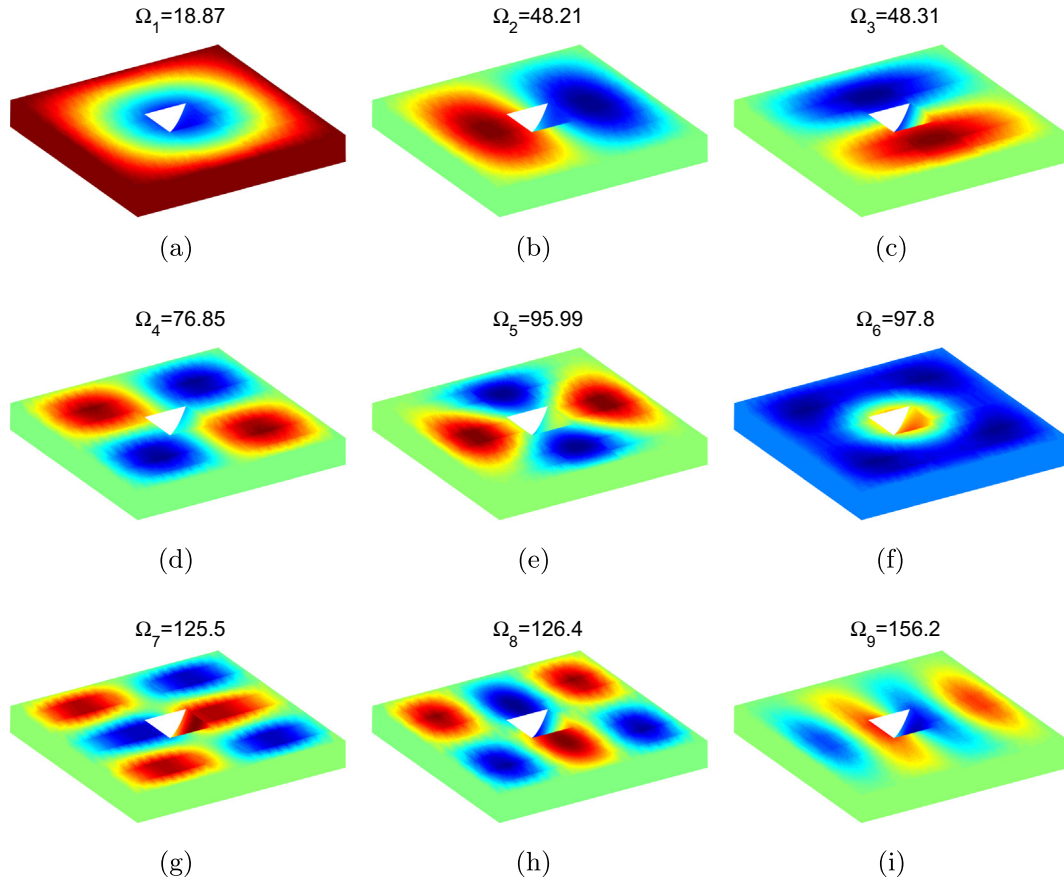
Fig. 4. Mode shapes for increasing natural frequencies of a square plate with a square hole filled with a double quadratic power-law profile section. The size of the profile is $a_1/a = 0.2$ where the truncation points are given by $(x_{2t} - x_{1t})/a = 0.1a_1/a$. Note dimensions not to scale.
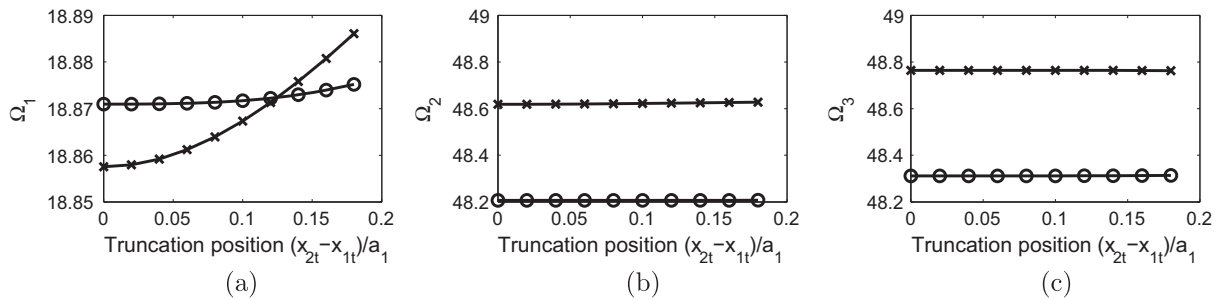
Fig. 5. Variation of natural frequencies with a variation in the truncation position for a square plate. The outer size of the inclusion is $a_1/a = 0.2$, with the power-law of the profile being $-x$ linear and $-o$ quadratic, for (a) Ω_1, (b) Ω_2, and (c) Ω_3.

The properties of the viscoelastic damping layer reflect a material such as butyl rubber, with thickness $h_d = 1$ mm, Young's modulus $E_d = 15$ MPa and loss factor $\eta_d = 0.8$, where the loss factor is incorporated into the numerical prediction through making the Young's modulus complex, $E'_d = E_d(1 + i\eta_d)$. By fully attaching the damping layer to a steel sheet, the overall composite loss factor η_{COMP} for flexural waves at any local position can be obtained (composite defined as steel and damping layer). Oberst [14] provides an approximation dependent on the extensional stiffness of the two layers as,

$$\eta_{COMP} = \frac{\eta_d \alpha [12\beta^2 + \Gamma^2(1 + \alpha)^2]}{[1 + \alpha][12\alpha\beta^2 + (1 + \alpha)(1 + \alpha\Gamma^2)]} \quad (12)$$

where the subscript p denotes plate material and d the damping material. The terms $\Gamma = h_d/h_p$, $\alpha = \Gamma E_d/E_p$ and $\beta = (h_d + h_p)/2h_p$.

Three test cases are shown as industrial examples. The first is a rectangular plate with a thin rectangular slot at the truncation positions. The only damping is the inherent metal damping. This is termed the "plain plate". The second case is the plain plate with a layer of damping material of thickness 1 mm applied to the whole surface, termed the "plain damped". Finally the last case shown is the rectangular plate with a double quadratic profile extending to the truncation positions, which has a layer of damping material on top. This is termed the "profiled plate".

All three cases are illustrated as cross-sections on the left-hand side of Fig. 7 (note axes not to scale). On the right-hand side are the

Table 5
First natural frequency Ω_1 for a rectangular plate with profiled inner double linear profile where $b < a$. Variation of the size of the outer profile and truncation length.

b/a	a_1/a	$(x_{2t} - x_{1t})/a_1$					
		0.00	0.05	0.10	0.15	0.20	0.25
0.600	0.10	36.724	36.725	36.728	36.733	36.739	36.745
	0.17	35.856	35.859	35.868	35.883	35.902	35.922
	0.20	35.391	35.396	35.410	35.433	35.461	35.493
	0.30	34.146	34.159	34.195	34.253	34.326	34.415
	0.33	33.812	33.828	33.875	33.949	34.044	34.159
	0.40	33.281	33.307	33.381	33.496	33.648	33.833
	0.50	32.737	32.785	32.919	33.127	33.402	33.733
0.700	0.10	29.604	29.605	29.607	29.611	29.616	29.621
	0.17	28.966	28.969	28.976	28.988	29.002	29.019
	0.20	28.627	28.631	28.642	28.660	28.682	28.707
	0.30	27.734	27.744	27.773	27.818	27.876	27.946
	0.33	27.503	27.516	27.553	27.611	27.686	27.778
	0.40	27.152	27.173	27.231	27.322	27.443	27.593
	0.50	26.837	26.875	26.981	27.146	27.367	27.636
0.800	0.10	24.967	24.967	24.969	24.973	24.977	24.981
	0.17	24.453	24.455	24.462	24.471	24.483	24.497
	0.20	24.181	24.185	24.194	24.208	24.227	24.247
	0.30	23.472	23.480	23.504	23.541	23.589	23.648
	0.33	23.292	23.303	23.334	23.382	23.444	23.521
	0.40	23.028	23.045	23.094	23.169	23.270	23.396
	0.50	22.814	22.846	22.933	23.071	23.257	23.485
0.900	0.10	21.776	21.777	21.779	21.781	21.785	21.789
	0.17	21.331	21.333	21.338	21.346	21.357	21.368
	0.20	21.094	21.097	21.105	21.118	21.133	21.151
	0.30	20.478	20.485	20.506	20.537	20.578	20.629
	0.33	20.322	20.332	20.358	20.399	20.452	20.519
	0.40	20.094	20.109	20.151	20.215	20.302	20.412
	0.50	19.916	19.943	20.018	20.136	20.298	20.497

Table 7
First natural frequency Ω_1 for a rectangular plate with profiled inner double quadratic power-law profile where $b < a$. Variation of the size of the outer profile and truncation length.

b/a	a_1/a	$(x_{2t} - x_{1t})/a_1$					
		0.00	0.05	0.10	0.15	0.20	0.25
0.600	0.10	36.604	36.604	36.605	36.605	36.607	36.609
	0.17	35.668	35.669	35.669	35.672	35.676	35.683
	0.20	35.211	35.211	35.212	35.216	35.222	35.233
	0.30	34.213	34.214	34.217	34.226	34.244	34.272
	0.33	34.044	34.045	34.049	34.062	34.085	34.122
	0.40	33.956	33.957	33.966	33.988	34.028	34.089
	0.50	34.321	34.325	34.348	34.402	34.492	34.621
0.700	0.10	29.528	29.528	29.528	29.529	29.530	29.531
	0.17	28.864	28.864	28.865	28.867	28.870	28.876
	0.20	28.546	28.546	28.547	28.550	28.555	28.563
	0.30	27.901	27.902	27.905	27.912	27.926	27.948
	0.33	27.821	27.822	27.825	27.835	27.854	27.883
	0.40	27.870	27.871	27.878	27.895	27.926	27.975
	0.50	28.381	28.383	28.399	28.439	28.507	28.607
0.800	0.10	24.914	24.914	24.914	24.914	24.915	24.917
	0.17	24.396	24.396	24.397	24.398	24.401	24.406
	0.20	24.152	24.152	24.153	24.155	24.159	24.166
	0.30	23.685	23.685	23.688	23.694	23.705	23.724
	0.33	23.645	23.645	23.648	23.656	23.672	23.696
	0.40	23.745	23.746	23.751	23.765	23.791	23.832
	0.50	24.284	24.286	24.299	24.331	24.386	24.468
0.900	0.10	21.736	21.736	21.736	21.736	21.737	21.739
	0.17	21.298	21.298	21.299	21.300	21.302	21.306
	0.20	21.093	21.093	21.094	21.096	21.099	21.105
	0.30	20.710	20.711	20.713	20.718	20.728	20.744
	0.33	20.684	20.685	20.687	20.694	20.708	20.729
	0.40	20.792	20.793	20.798	20.810	20.832	20.867
	0.50	21.305	21.307	21.317	21.344	21.390	21.461

Table 6
First natural frequency Ω_1 for a rectangular plate with profiled inner double linear profile where $b > a$. Variation of the size of the outer profile and truncation length.

b/a	a_1/a	$(x_{2t} - x_{1t})/a_1$					
		0.00	0.05	0.10	0.15	0.20	0.25
1.100	0.10	17.786	17.786	17.788	17.790	17.793	17.796
	0.17	17.391	17.393	17.397	17.404	17.412	17.421
	0.20	17.180	17.183	17.189	17.199	17.211	17.224
	0.30	16.616	16.622	16.638	16.663	16.695	16.735
	0.33	16.469	16.477	16.498	16.530	16.572	16.625
	0.40	16.243	16.255	16.288	16.338	16.407	16.496
	0.50	16.045	16.067	16.125	16.219	16.348	16.509
1.200	0.10	16.488	16.488	16.490	16.492	16.494	16.497
	0.17	16.097	16.099	16.103	16.109	16.116	16.124
	0.20	15.887	15.889	15.895	15.904	15.915	15.926
	0.30	15.316	15.321	15.337	15.359	15.387	15.424
	0.33	15.164	15.171	15.190	15.219	15.257	15.306
	0.40	14.922	14.933	14.963	15.009	15.072	15.153
	0.50	14.695	14.715	14.768	14.852	14.971	15.119
1.300	0.10	15.474	15.474	15.476	15.477	15.480	15.482
	0.17	15.079	15.081	15.085	15.090	15.097	15.104
	0.20	14.866	14.868	14.873	14.882	14.891	14.902
	0.30	14.278	14.283	14.297	14.317	14.343	14.376
	0.33	14.118	14.124	14.142	14.168	14.203	14.248
	0.40	13.856	13.866	13.894	13.936	13.994	14.070
	0.50	13.594	13.612	13.661	13.739	13.848	13.986
1.400	0.10	14.666	14.667	14.668	14.670	14.672	14.674
	0.17	14.263	14.264	14.268	14.273	14.279	14.285
	0.20	14.043	14.045	14.051	14.058	14.067	14.076
	0.30	13.432	13.437	13.450	13.469	13.493	13.523
	0.33	13.262	13.268	13.285	13.309	13.342	13.384
	0.40	12.979	12.988	13.014	13.052	13.107	13.178
	0.50	12.681	12.697	12.742	12.814	12.916	13.045

Table 8
First natural frequency Ω_1 for a rectangular plate with profiled inner double quadratic power-law profile where $b > a$. Variation of the size of the outer profile and truncation length.

b/a	a_1/a	$(x_{2t} - x_{1t})/a_1$					
		0.00	0.05	0.10	0.15	0.20	0.25
1.100	0.10	17.756	17.756	17.756	17.757	17.757	17.758
	0.17	17.380	17.380	17.380	17.381	17.383	17.387
	0.20	17.201	17.202	17.202	17.204	17.207	17.212
	0.30	16.855	16.855	16.857	16.861	16.869	16.882
	0.33	16.822	16.822	16.824	16.830	16.841	16.858
	0.40	16.888	16.888	16.892	16.902	16.919	16.948
	0.50	17.284	17.285	17.293	17.313	17.349	17.405
1.200	0.10	16.460	16.460	16.460	16.460	16.461	16.462
	0.17	16.090	16.090	16.090	16.091	16.093	16.096
	0.20	15.912	15.912	15.912	15.914	15.917	15.921
	0.30	15.551	15.551	15.553	15.557	15.564	15.576
	0.33	15.507	15.507	15.509	15.514	15.524	15.540
	0.40	15.541	15.541	15.545	15.553	15.570	15.596
	0.50	15.868	15.869	15.876	15.895	15.928	15.979
1.300	0.10	15.447	15.447	15.447	15.447	15.447	15.448
	0.17	15.073	15.073	15.074	15.075	15.076	15.079
	0.20	14.892	14.892	14.893	14.894	14.897	14.901
	0.30	14.508	14.508	14.509	14.513	14.520	14.532
	0.33	14.450	14.451	14.452	14.457	14.467	14.482
	0.40	14.450	14.451	14.454	14.462	14.477	14.501
	0.50	14.709	14.710	14.717	14.733	14.764	14.811
1.400	0.10	14.638	14.638	14.639	14.639	14.639	14.640
	0.17	14.257	14.257	14.257	14.258	14.260	14.263
	0.20	14.070	14.070	14.070	14.071	14.074	14.078
	0.30	13.657	13.657	13.658	13.662	13.669	13.679
	0.33	13.585	13.586	13.587	13.592	13.601	13.615
	0.40	13.551	13.551	13.554	13.562	13.576	13.599
	0.50	13.744	13.744	13.751	13.766	13.795	13.839

Fig. 6. Illustration of a typical automotive panel (bonnet shown) with holes for weight saving and attachment of the heavy trim liner (bottom of the photo). Automotive bulkheads typically have access holes for cables and heating ducts. Typical solutions for noise and vibration include attachment of viscoelastic damping layers.

composite loss factors for every position on the cross section. For the plain plate, only inherent damping $\eta = 0.01$ is present. For the plain plate with damping layer, the composite damping rises to $\eta_{COMP} = 0.0101$ (an increase of only 1%) as the plate properties dominate Eq. (12). This shows the relative futility of covering the whole plate with damping material, as is the usual solution to plate vibration problems.

The composite damping when applied to the profile shows a significant rise close to the truncation point. Any flexural waves which have a sufficiently high wavelength will be able to propagate into the profile and be attenuated. Indeed, such is the lack of impact covering the constant thickness sections, it would make as much sense to just apply damping to the tapering thickness areas.

This composite loss factor, which varies according to position on the structure, leads to an overall modal loss factor for each natural frequency. The damped natural frequency λ_r for the r_{th} mode is related to the undamped natural frequency ω_r and the modal loss factor η_r through $\lambda_r^2 = \omega_r^2(1 + i\eta_r)$ (with associated non-dimensional parameter $\bar{\Omega}_r$).

The damped natural frequency and the modal loss factors are shown in Table 9 for the three case studies. It can be seen that when the mode shape indicates an incident angle for the flexural wave into the profiled section which is large, the modal loss factor is relatively low (yet still higher than for the constant thickness plate). However, for higher modes, the profiled plate shows a more significant and more effective increase in the modal damping. This is consistent with shorter wavelength flexural waves propagating into the tapering section where the damping layer is then forced to extend and compress significantly.

The mass of the damping material for the damped plain plate and profiled plates are approximately equal, however, the mass of damping material could be further reduced by not covering the constant thickness sections of the profiled plate, as these parts do not generate a significant reduction in amplitude. Along with an appreciable increase in the modal damping, the reduction in damping mass will lead to financial and carbon cost reductions. It is a simple step to generate the frequency response functions for the forced case through a modal summation, to obtain the point
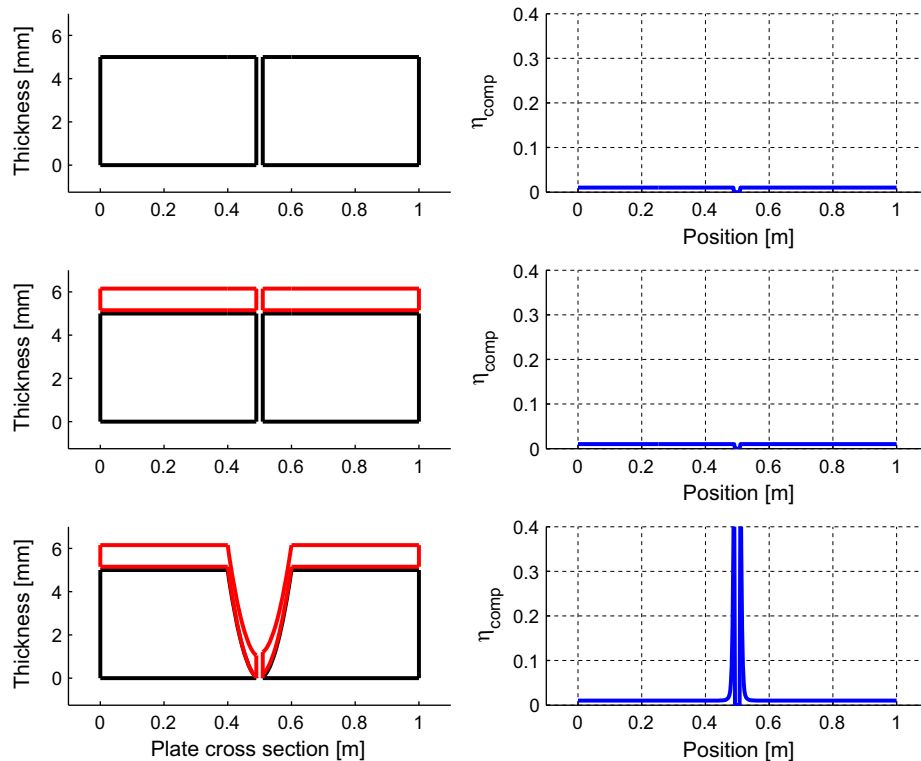
Fig. 7. Three industrial cases compared, a plain plate with only inherent damping (top), the same with a layer of damping tape applied (middle) and a plain plate with a damped profiled indentation (bottom). Cross sections through the material are shown on the left and the composite damping at each position on the right.

Table 9
Comparison of three test cases for enhanced damping in a plate structure with an access hole. Damped natural frequencies $\bar{\Omega}_r$ for different modes r, with associated modal loss factor η_r %.

Mode number	Plain plate	Plain damped	Profiled plate
1	49.24 (1.00)	49.24 (1.02)	44.38 (1.11)
2	78.92 (1.00)	78.92 (1.02)	76.07 (1.06)
3	127.72 (1.00)	127.72 (1.02)	129.16 (1.03)
4	167.51 (1.00)	167.51 (1.02)	135.40 (1.19)
5	196.74 (1.00)	196.74 (1.02)	181.87 (1.10)
6	197.33 (1.00)	197.33 (1.02)	187.48 (1.06)
7	246.66 (1.00)	246.66 (1.02)	227.36 (1.06)
8	284.50 (1.00)	284.50 (1.02)	281.17 (1.08)
9	314.22 (1.00)	314.22 (1.02)	296.69 (1.07)
10	365.26 (1.00)	365.26 (1.02)	317.76 (1.77)
11	394.24 (1.00)	394.24 (1.02)	352.58 (1.28)
12	394.77 (1.00)	394.77 (1.02)	380.88 (1.05)
13	404.63 (1.00)	404.63 (1.02)	383.59 (1.05)
14	444.94 (1.00)	444.94 (1.02)	390.59 (1.33)
15	511.03 (1.00)	511.03 (1.02)	454.21 (1.23)
16	511.78 (1.00)	511.78 (1.02)	455.68 (1.41)
17	520.98 (1.00)	520.98 (1.02)	484.62 (1.08)
18	603.89 (1.00)	603.90 (1.02)	513.88 (1.79)
19	639.35 (1.00)	639.35 (1.02)	523.31 (1.36)
20	642.46 (1.00)	642.46 (1.02)	528.80 (1.06)

mobility of each plate, where the larger modal loss factor would lead to a reduction in vibration amplitude.

5. Conclusions

It has been shown that the natural frequencies of vibration of a complex plate structure can be approximately determined using a variational Rayleigh–Ritz method. The plate is a square or rectangular structure of constant thickness incorporating a central double profiled indentation of power-law profile (linear or quadratic). The size of the truncation position of the power-law profile can be moved to alter the size of the inner aperture.

The natural frequencies have been predicted for a range of plate dimensions and truncation sizes using a variational Rayleigh–Ritz method incorporating 30 terms, sufficient to resolve the change in natural frequency with subsequent additional terms to within one percent. The numerical model has been validated in sections against numerical predictions published in the literature with excellent agreement against finite element calculations. It has been shown that a plate with a double linear power-law profile has a higher natural frequency than a similar plate with a quadratic power-law indentation for small profile sizes.

The method is sufficiently adaptable to allow the movement of the aperture to any location on the plate and many other thickness variations can be employed provided the numerical integrals can be completed.

A demonstration of the use of tapered indentations as highly efficient damping mechanisms for flexural waves has been shown.

Acknowledgement

References

[1] Grootenhuis P. The control of vibrations with viscoelastic materials. J. Sound Vib. 1970;11(4):421–33.
[2] Sasajima M, Kakudate T, Narita Y. Vibration behavior and simplified design of thick rectangular plates with variable thickness. Journal of Vibration and Acoustics (ASME) 2002;124:302–9.
[3] Leissa AW. Vibration of plates. NASA SP160. Washington, D.C.: US Government Printing Office; 1969.
[4] Leissa AW. Vibration of shells. NASA SP288. Washington, D.C.: U.S. Government Printing Office; 1973.
[5] Liew KM, Xiang Y. Kitipornchai, Research on thick plate vibration: a literature survey. J. Sound Vib. 1995;180:163–76.
[6] Chen D-Y, Ren B-S. Finite element analysis of the lateral vibration of thin annular and circular plates with variable thickness. Journal of Vibration and Acoustics (ASME) 1998;120(3):747–52.
[7] Chakraverty S, Jindal R, Agarwal VK. Vibration of nonhomogeneous orthotropic elliptical and circular plates with variable thickness. Journal of Vibration and Acoustics (ASME) 2007;129:256–9.
[8] O'Boy DJ, Krylov VV, Kralovic V. Damping of flexural vibrations in rectangular plates using the acoustic black hole effect. J. Sound Vib. 2010;329 (22):4672–88.
[9] O'Boy DJ, Krylov VV. Damping of flexural vibrations in circular plates with tapered central holes. J. Sound Vib. 2011;330(10):2220–36.
[10] Cranch E, Adler A. Bending vibrations of variable section beams. J. Appl. Mech. 1956;23(1):103–8.
[11] Mironov MA. Propagation of a flexural wave in a plate whose thickness decreases smoothly to zero in a finite interval. Soviet Physics - Acoustics 1988;34:318–9.
[12] Krylov VV, Tilman FJBS. Acoustic 'black holes' for flexural waves as effective vibration dampers. J. Sound Vib. 2004;274(3-5):605–19.
[13] Krylov VV. New type of vibration dampers utilising the effect of acoustic 'black holes'. Acta Acustica united with Acustica 2004;90(5):830–7.
[14] Ross D, Kerwin EM, Ungar EE. Damping of plate flexural vibrations by means of viscoelastic laminae. In: Ruzicka JE, editor. Structural Damping, vol. 3. Oxford: Pergamon; 1960. p. 49–87.
[15] Ungar EE. Loss factors of viscoelastically damped beam structures. J. Acoust. Soc. Am. 1962;34(8):1082–9.
[16] Heckl M, Cremer L, Ungar EE. Structure Borne Sound. 2nd ed. Berlin: Springer-Verlag; 1988.
[17] Mead DJ. Passive Vibration Control. Chichester: Wiley & Sons; 1998.
[18] Mansfield EH. On the analysis of elastic plates of variable thickness. Q. J. Mech. Appl. Mech. 1962;15(2):167–92.
[19] Trapezon AG. Natural vibrations and the stress state of a beam with thickness varying according to an exp(ax∗∗2) rule. Strength Mater. 1980;12(1):98–103.
[20] Lardner TJ. Vibration of beams with exponentially varying properties. Acta Mech. 1968;6(1):197–202.
[21] Wang HG. Generalized hypergeometric function solutions on the transverse vibration of a class of non-uniform beams. J. Appl. Mech. 1967;34(1):702–8.
[22] Jain RK, Soni SR. Free vibrations of rectangular plates of parabolically varying thickness. Indian Journal of Pure and Applied Mathematics 1973;4(3):262–77.
[23] Tomar JS, Gupta DC, Jain NC. Free vibrations of an isotropic nonhomogeneous infinite plate of linearly varying thickness. Meccanica 1983;18(1):30–3.
[24] Young D. Vibration of rectangular plates by the Ritz method. J. Appl. Mech. 1950;17:448–52.
[25] Warburton GB. The vibration of rectangular plates. Proceedings of the Institution of Mechanical Engineers, Serial A. 1954;168:371–84.
[26] Gupta AP, Bhardwaj N. Vibration of rectangular orthotropic elliptic plates of quadratically varying thickness resting on elastic foundation. Journal of Vibration and Acoustics (ASME) 2004;126:132–40.
[27] Laura PAA, Laura PA, Cortinez VH. A note on transverse vibrations of a rectangular plate with a free, rectangular corner cut-out. J. Sound Vib. 1986;106(2):187–92.
[28] Laura PAA, Romanelli E, Rossi RE. Transverse vibrations of simply supported rectangular plates with rectangular cutouts. J. Sound Vib. 1997;202 (2):275–83.
[29] Avalos DR, Laura PAA. Transverse vibrations of simply supported rectangular plates with two rectangular cutouts. J. Sound Vib. 2003;267(1):967–77.
[30] Warburton GB. Response using the Rayleigh-Ritz method. Earthquake Eng. Struct. Dynam. 1979;7:327–34.
[31] Larrondo HA, Avalos DR, Laura PAA, Rossi RE. Vibrations of simply supported rectangular plates with varying thickness and same aspect ratio cutouts. J. Sound Vib. 2001;244(4):738–45.
[32] Nallim LG, Luccioni BM, Grossi RO. A Rayleigh-Ritz approach to transverse vibration of isotropic polygonal plates with variable thickness, Proceedings of the Institution of Mechanical Engineers. Part K: Journal of Multi-body Dynamics 2002;216(3):213–22.
[33] Laura PAA. Static and dynamic behavior of circular plates of variable thickness elastically restrained along the edges. J. Sound Vib. 1997;52(2):243–51.
[34] Zhou D. Vibrations of point-supported rectangular plates with variable thickness using a set of static tapered beam functions. Int. J. Mech. Sci. 2002;44(1):149–64.